Title
ANTIPROTON ANNIHILATION AT REST IN DEUTERIUM

Authors
Chinowsky, W.
Kojoian, G.

Publication Date
1965-11-03

UCRL-16335

University of California

Ernest O. Lawrence Radiation Laboratory

ANTIPROTON ANNIHILATION AT REST IN DEUTERIUM

Berkeley, California

DISCLAIMER

Submitted to Il Nuovo Cimento

UCRL-16335

UNIVERSITY OF CALIFORNIA

Lawrence Radiation Laboratory
Berkeley, California

AEC Contract No. W-7405-eng-48

ANTIPROTON ANNIHILATION AT REST IN DEUTERIUM

W. Chinowsky and G. Kojoian

November 3, 1965

ANTIPROTON ANNIHILATION AT REST IN DEUTERIUM*

W. Chinowsky and G. Kojoian†

Lawrence Radiation Laboratory
University of California
Berkeley, California

November 3, 1965

SUMMARY

Annihilation of antiprotons at rest in the Lawrence Radiation Laboratory's 15-inch deuterium-filled bubble chamber has been studied. Particular emphasis was on investigation of the characteristics of the antiproton-neutron annihilations. With a total of 2071 observed events, the ratio of the number of annihilations on protons to that on neutrons was found to be 1.33 ± 0.07. The observed momentum distribution of proton recoils accompanying the neutron-annihilation products deviates strongly from the deuterium internal-momentum distribution and cannot be explained by final-state pion-proton interactions. Three-body effects are considered. Multiplicity and momentum distributions of the annihilation products are in agreement with predictions of a Lorentz-invariant phase-space model with an interaction volume of radius about 2.2 pion-Compton-wavelengths. Annihilations yielding K mesons accounted for 0.05 ± 0.01 of the neutron annihilations.

1. Introduction.

The antiproton-annihilation process at rest has been extensively studied in heavy elements[1,2], and in hydrogen[3,4]. The results show a dominance of statistical factors. An important conclusion for the understanding of the dynamics of the annihilation is that in proton annihilations at rest, essentially all absorption takes place in the S state of protonium. This is the only "selection rule" established as yet. A possible dependence on isotopic spin can be established by studying the characteristics of the antiproton-neutron annihilation. To this end, we present here some features of antiproton-deuteron annihilations[5].

2. Experimental arrangement.

A separated beam[6] of 790-MeV/c antiprotons was slowed down by suitable absorbers and brought to rest in the Lawrence Radiation Laboratory 15-inch deuterium-filled bubble chamber in a magnetic field of 12.3 kilogauss. The intensity of the beam was 1 $\bar{p}$ per 12 pictures with a background of ≈ 1 light track per picture. A total of 40 000 photographs yielded 2578 annihilation events within a restricted fiducial volume of the chamber, so chosen that tracks in a well-illuminated portion of the chamber were long enough for estimating bubble density and thus identifying protons among the annihilation products. All film was scanned twice and all events were measured with a digitized measuring projector, "Franckenstein." Background tracks were easily separated from the much more heavily ionizing antiproton tracks, and thus were not a source of confusion.

3. Results: Annihilations at rest.

3.1 Ratio of neutron to proton annihilations.—Annihilations produced by antiprotons at rest in deuterium represent, in fact, the great majority of

observed events. Such events were selected by requiring consistency of the measured initial momentum of the incoming antiproton with that inferred from the length of the track. All events with the measured $\bar{p}$ momentum within two standard deviations of the momentum inferred from range were included in this sample. The scatter plot of Fig. 1, showing the inverse of initial momentum vs length of track, clearly indicates a strong clustering of events near the locus expected for interactions of particles at rest. It is estimated from this plot that our sample of 2071 events at rest, of a total of 2578 events, includes less than 5% events in flight. Events with identified strange particles, not included here, are discussed separately below.

Of these annihilations at rest, 468 events had an odd number of charged prongs with total charge -1. These events presumably also include a recoil proton of momentum $\lesssim$ 80 MeV/c, insufficient to produce an observable track. Deferring the question of possible three-body annihilation effects, we consider these unambiguous examples of antiproton-neutron annihilations. In addition, among the events with zero total charge in outgoing prongs, 263 had positive tracks which stopped in the chamber and were identified as proton recoils. Further, 159 contained a proton identified on the basis of bubble density; this type is subject to error due to possible inclusion of pion tracks with large dip angle and of K^+ tracks. The distribution in dip angle of these tracks is, however, quite consistent with that expected from isotropy. Indeed, only 10 of the proton tracks had dip angles greater than 70°. The contamination of pions in this sample is thus considered negligible. It is known[4] that K mesons are produced in 6.8% of $\bar{p}p$ annihilations at rest. Assuming that $\approx$ one half of such stars yield positive K mesons, we expect than some 40 K^+'s to be produced. Of these, only those with momenta from about 300 to 500 MeV/c might be confused with protons. A phase-space distribution of momenta implies that

in this region will occur about 40% of the total of positive K mesons produced, so that perhaps 16 K^+'s are possible contaminants. In fact, 10 K^+'s were identified in this momentum region, so we estimate 6 ± 3 K^+'s included in the sample of tracks called protons, distributed approximately uniformly from 300 to 500 MeV/c. Thus, the observed spectrum is not much distorted by the inclusion of misidentified positive K mesons.

With these 890 examples of annihilations on neutrons and 1181 on protons, we obtain for the ratio of annihilation rates $R(\bar{p}p)/R(\bar{p}n) = 1.33 \pm 0.07$, including 62 zero-prong events. This result is insensitive to effects of pion-nucleon final-state interactions. Charge-exchange reactions $\pi^- p \rightarrow \pi^0 n$ and $\pi^0 p \rightarrow \pi^+ n$ cause a neutron annihilation to simulate a proton absorption, whereas the opposite is true of the reactions $\pi^0 n \rightarrow \pi^- p$ and $\pi^+ n \rightarrow \pi^0 p$. All these reactions may be expected to proceed at approximately equal rates. The overall n-p "exchange" rates may then be qualitatively estimated for the five-pion state, the dominant configuration. With the assumption of a statistical distribution of charges[7], the $\bar{p}p$ annihilation yields, on the average, 1.6 π^+'s, 1.6 π^-'s, and 1.8 π^0's, and the $\bar{p}n$ annihilation yields 1.2 π^+'s, 2.2 π^-'s, and 1.6 π^0's. With these fluxes the neutron-proton exchange is essentially zero. A more realistic calculation can not be expected to yield much more than a few percent effect, since it is known that deviations from the statistical model are not large.

This ratio of the rates of proton to neutron annihilations is determined by the isotopic-spin dependence of the annihilation matrix element, because the $\bar{p}p$ system is an equal mixture of $T = 0$ and $T = 1$ states but the $\bar{p}n$ system is $T = 1$ only. The complexity of the situation unfortunately precludes the possibility of an unambiguous determination of the relative rates of annihilation in the two isotopic-spin states. If one makes the simplest assumption—that the

$\bar{p}p$ rate is a statistical sum of the T = 0 and T = 1 rates—then one sees that $R(\bar{p}p) = 1/2\ R(T=0) + 1/2\ R(T=1)$, and the $\bar{p}n$ annihilation rate $R(\bar{p}n) = R(T=1)$. For annihilation into a state of n pions, the relative rate, within the framework of the statistical model[8], is then:

$$\rho_n \equiv \frac{R_n(\bar{p}p)}{R_n(\bar{p}n)} = \frac{1/2\ N_n(T=0)\left|M_n(0)\right|^2 + 1/2\ N_n(T=1)\left|M_n(1)\right|^2}{N_n(T=1)\left|M_n(1)\right|^2},$$

where $M_n(0)$ and $M_n(1)$ represent effective matrix elements for transitions in the T = 0 and T = 1 states, averaged over the various final-state configurations. The weight factors $N_n(T=0)$ and $N_n(T=1)$ are the number of linearly independent states constructed of n pions, these states being characterized only by the total isotopic spin. Since attempts to calculate such factors in modified statistical models including conservation laws other than momentum and energy[8] have not been successful, we use a simple enumeration of the number of such states independent of the quantum numbers (other than isotopic spin) characterizing the particular configurations. These are listed in Table I[9]. If the matrix elements were independent of isotopic spin, the statistical ratios, ρ_{stat}, shown in Table I, would follow. It is seen then that ρ_{stat} is relatively independent of n, so that a net ratio $\rho_{stat} = 0.71$ would be expected; this ratio is inconsistent with the observed one. From the result above, $\rho = 1.33$, we conclude that $R(T=0) = 1.66\ R(T=1)$.

The applicability of a simple statistical model is, of course, quite dubious, as is also the naive description of deuterium annihilations in terms of two-body annihilations. Further, the effect of the $\bar{p}p$ Coulomb attraction may be expected to increase the proton annihilations. The significance of this result is therefore somewhat obscure. Note, however, that a similar

TABLE I. Ratio for annihilations into n pions.

N	N(0)	$N_n(1)$	ρ_{stat}
2	1	1	1.0
3	1	3	0.67
4	3	6	0.75
5	6	15	0.70
6	15	36	0.71
7	36	91	0.70

conclusion—annihilation from T = 0 states dominates—has been drawn from observation of the process $\bar{p} + p \rightarrow \rho^0 + \pi^0$ by CHADWICK et al.[10].

3.2. Prong multiplicity and momentum distributions.—The multiplicity distribution of the observed charged prongs is shown in Fig. 2. The average number of charged pions in the proton annihilations is 3.03 ± 0.10; in the neutron annihilations it is 3.11 ± 0.12. In common with earlier results on $\bar{p}$-p and $\bar{p}$-nucleus annihilation[1-4], these distributions require a large interaction volume to be in agreement with predictions of the statistical model. Again, an interaction volume with radius about 2.2-pion-Compton wavelengths yields results in agreement with observation.

Momentum distributions of the charged pions resulting from the observed neutron annihilations are shown in Figs. 3 and 4. Corresponding momentum distributions of prongs from proton annihilations are essentially identical to those observed in antiproton annihilation on free protons[3,4], and so are not shown here. We emphasize that we have plotted the momenta calculated directly from the measured track curvatures, without using the common technique of adjusting measured quantities to obtain a statistically best fit to the kinematic equations of energy and momentum conservation. This procedure, for almost all the events here, did not unambiguously determine the number of unobserved neutral particles produced in the annihilation. The measured quantities could not, therefore, be constrained by the conservation equations. For this reason the errors assigned to the momenta of the prongs are rather large, on the average $\pm 15\%$, and vary greatly with position in chamber, dip angle, and length of track. In making the distributions of Figs. 3 and 4, no restrictions were put on track quality, but all events were included which showed a measurable curvature.

Plotted in the figures are the momentum distributions expected from the statistical model mentioned above for annihilation on neutrons at rest. The agreement is rather good for both the three-prong and five-prong annihilations. In a few cases there resulted pions with momentum greater than that kinematically allowed in annihilation at rest. Because of the poor measurement accuracy, we cannot conclude, however, that these resulted from three-body annihilations, or from high-momentum components of the neutron internal-momentum distribution in the deuteron. Indeed, without exception these tracks were of very poor quality, and their uncertainties were so large that the measured momenta are consistent with being less than the indicated kinematical upper limit. Thus we are not able from these distributions to estimate the fraction of deuterium annihilations that should be considered examples of three-body interactions.

Results of a search for pion-pion correlations among the annihilation products are shown in the effective-mass distributions of Fig. 5. Again, in the calculations of effective mass we used measured, not fitted, quantities and so the mass resolution is poor. Also, because of the difficulties in fitting to particular hypotheses of number of particles, it was not feasible to search for unstable particles with neutral decay products. No significant deviations from the phase-space distribution of Fig. 5 are noted, so resonant-state production is small. It is clearly not possible to put meaningful quantitative limits on ρ^0 or f^0 production in these annihilations because of the poor mass resolution and the limited statistical accuracy.

3.3. Five-prong annihilations and selection rules. —It has been demonstrated that antiproton annihilations at rest in hydrogen proceed predominantly from S states[4]. As pointed out by BERMAN and OAKES[11], this

fact may imply that antiproton annihilation proceeds via an intermediate vector meson. If this rule is generally valid, the process $\bar{p} + n \rightarrow$ [odd number of pions] is forbidden.

To test this hypothesis we analyzed events with five charged pions and visible proton recoil to determine the number of neutral pions produced. A total of 67 such events were fitted to the hypotheses that the final state contained zero or one neutral pion, these being four constraint and one constraint fits, respectively. We separated the two groups on the basis of goodness-of-fit and missing-mass values. Chi-squared distributions are shown in Fig. 6 for 15 events classified as examples of $\bar{p}d \rightarrow 3\pi^- + 2\pi^+ + p$ and 39 of $3\pi^- + 2\pi^+ + \pi^0 + p$. In Fig. 7 we plot the distribution in the missing mass for all the five-prong annihilations, showing the separation of events classified as having zero, one, and two-or-more π^0's. We find $0\pi^0/1\pi^0/\geq 2\pi^0$ to be equal to 15/39/13. The corresponding prediction of the statistical model with interaction radius $r = 2.15\,\lambda\!\!\!^{-}_{\pi}$ is 26/33/8, if contributions from states with more than seven pions are neglected. The observation deviates from the statistical prediction but the disagreement is not overwhelming. In particular, it is clear that events with a single π^0 are not highly forbidden. It would appear that annihilation via an intermediate vector meson is not the only process involved in the $\bar{p}$-n interaction. Because of the motion of the neutron in the deuteron, these annihilations are not at rest; therefore, some p-state annihilation may be expected and the relevance of the model is somewhat obscure.

3.4. Proton-momentum distribution. —This discussion has proceeded on the assumption that effects of the presence of the second nucleon do not contribute to the annihilation dynamics. We may then expect the momentum

spectrum of protons from the reaction $\bar{p} + d \rightarrow n\pi + p$ to have a shape corresponding to the deuteron-momentum-space wavefunction. In Fig. 8 we show the observed distribution for those protons resulting from the annihilations into three and five charged pions. Events with single pions have not been included because that group is more subject to bias in favor of higher momenta due to inclusion of misidentified positive pions among the much more numerous two-prong annihilations. Also plotted for comparison is the momentum distribution calculated from the phenomenological ground-state deuteron wavefunction of ERIKSSON, HULTHÉN, and JOHANSONS[12]. The observed shape is in poor agreement with this deuteron's internal-momentum distribution, with an impressively large excess of high-momentum protons. As a measure of the deviation, note that of the 732 protons included, 165 had momenta greater than 200 MeV/c, although only 40 are predicted on the basis of the "Hulthén" function. As discussed in Section 1, this distorted shape cannot be accounted for by a background of misidentified annihilation products. We conclude that the simple impulse-approximation model, with the second nucleon a spectator to the annihilation interaction, does not completely describe the $\bar{p}$-deuteron annihilation process.

We consider how some secondary effects in an attempt to understand the shift toward high momentum.

3.4.1. Final-state interactions – nucleon isobar production. —To estimate the effect of the resonant π^+-p interaction in the final state, we applied a theoretical model of GILLESPIE[13] to the particular reaction $\bar{p} + d \rightarrow 5\pi + p$. A detailed discussion of the technique used to calculate the proton spectrum is given in the Appendix. The essential point is the assumption that the primary reaction proceeds according to the statistical model with

the initial neutron momentum taken into account and overall energy-momentum balance required. The rate of annihilation into a particular final state is then weighted by a function of the pion momentum to strongly enhance the yield when the energy of the pion-proton system is near resonance. Our calculation overestimates the effect because the same weighting factors were used for all pions, independent of their charges. In Fig. 9 we show the results of the Monte Carlo calculation of the proton-momentum spectrum, including final-state interactions, together with the phenomenological deuteron internal-momentum distribution. The shapes are not much different, with no displacement toward higher momenta present in the distribution that includes effects of final-state interaction. Rather there is an enhancement near 140 MeV. It is perhaps tempting then to identify the deficiency of proton recoils in the region near 160 MeV/c (see Fig. 8) as an effect of the final-state interaction, but it is difficult to draw any conclusions about the shape of the spectrum below ≈ 150 MeV/c because of observational difficulties and serious measurement biases. In any event it appears that the excess of high-momentum protons does not result from the pion-proton interactions in the final state.

A different method of consideration of pion-proton interactions is to describe the annihilation as proceeding partly via the reaction

$$\bar{p} + d \rightarrow n\pi + N^{*}_{33} \longrightarrow p + \pi \ .$$

To calculate the proton spectrum resulting from the isobar decay, we have used a statistical model for isobar production and assumed isotropic decay of the excited nucleon. For the state of four pions and excited nucleon we obtained the spectrum shown in Fig. 10. Again quantitative agreement with the data is poor, although it is clear that isobar formation in three-body annihilations will yield

protons of very high momentum. Should such processes occur, the distribution of effective mass of pion-proton pairs may be expected to peak near 1238 MeV. Also, since the resonance is in T = 3/2 state, the $p\text{-}\pi^+$ state should be produced more copiously than the $p\text{-}\pi^-$ one. The observed distributions are shown in Fig. 11. No peaking is observed; the π^+p and π^-p effective-mass distributions are essentially identical. Since the phase-space effective-mass distribution peaks at ≈ 1200 MeV, the latter fact is considered more significant. These distributions are then consistent with zero isobar formation and indicate that this is not a major contributor to the annihilation.

3.4.2. Three-body antiproton interactions. —The initial state of antiproton and deuteron should be described by a wavefunction appropriate to the three-body system of antiproton, proton, and neutron. Then, in the spirit of the impulse approximation, the proton-momentum spectrum will be given by the corresponding momentum-space eigenfunction. To make such a calculation is a formidable, if not forbidding, task. Recently, progress has been made in the theoretical description of the bound state of three nucleons[14] with indications that simple functions may be used for the wavefunctions. Thus, a symmetric Gaussian form

$$\psi(\underset{\sim}{r}_1, \underset{\sim}{r}_2, \underset{\sim}{r}_3) = A \exp[-\tfrac{1}{2}\alpha^2(r_{12}^2 + r_{13}^2 + r_{23}^2)]$$

with $\underset{\sim}{r}_{ij} = \underset{\sim}{r}_i - \underset{\sim}{r}_j$ may be considered. It yields a nucleon momentum-space wavefunction also Gaussian in shape —$\psi(k) = \text{constant} \times \exp(-k^2/4\alpha^2)$. The momentum distribution is then given by

$$F(k) = k^2 \exp(-k^2/2\alpha^2).$$

Such a function will not fit the observed distribution. Its peak is at $k = \sqrt{2}\alpha$. Thus by appropriate choice of α we may account for a high-momentum tail superimposed on a "Hulthén" distribution. In the present case, an average two-nucleon separation $\bar{r} = 6 \times 10^{-14}$ cm in the three-body nucleus yields a peak in the nucleon-momentum spectrum at 300 MeV/c. Qualitatively we may say then that should the antinucleon cause a compaction of the initial system to distances of order 6×10^{-14} cm, recoil momenta of order 300 MeV/c are to be expected.

The simplest approach to the three-body system is again to use a statistical model to describe the process $\bar{p} + d \rightarrow p + n\pi$. To make definite predictions, an interaction radius, or equivalently an average multiplicity, must be assumed. It is sufficient for the annihilations being considered, into three and five charged prongs, for one to examine the distribution resulting from a five-pion annihilation, shown in Fig. 12. Again it is clear that the fit to the data is not good, although as before, we may perhaps assign the highest momenta as "three-body" annihilation products. For completeness we remark that the statistical model which yields agreement with the data, assuming the spectrum to be a simple sum of "two-body" and "three-body" distributions, would also lead to the prediction of annihilation into $\approx$ eight pions. In this case, the proton-momentum spectrum has a maximum at $P_p = 340$ MeV/c. It is difficult to reconcile such a dominant process with the lack of seven- and eight-prong events.

In concluding, we emphasize again that it is not possible to treat the three-body system rigorously, so the arguments about detailed shapes of the proton-recoil spectrum must be considered descriptive only. In this sense we cannot reject the notion that these high-momentum recoils, some 20% of

the events, result in some complicated manner from a simultaneous interaction of the antiproton with both nucleons.

If speculation is allowed, we suggest that the observed distribution may be considered the sum of three separate functions resulting from two-body annihilation, three-body annihilation, and also, in some fraction of the annihilations, from an initial state best described as a "bound" state of $\bar{p}$ and n, with a spectator proton. The annihilation is then that of the bound state, the recoil proton having the momentum appropriate to the reaction

$$\bar{p} + d \rightarrow [\bar{p}n]_{\text{bound}} + p$$

at rest. Giving the value P_p = 300 MeV/c, consistent with the spectrum of Fig. 8, we arrive at a mass of $M^* = 1803$ MeV for the $\bar{p}n$ system. With present theory it is not possible to rule out the possible existence of such a bound state, to estimate its binding energy, nor, in the present situation, to determine to what extent such an object would be formed; this then is a speculation suggested, but not required, by the data.

3.5. Strange-particle production. —Strange particles among the annihilation products were identified in 82 events. Among these were examples of observed K-meson pairs and single-K mesons, as listed in Table II, and six Λ^0 hyperons which, within the accuracy of measurement, appeared to originate at the annihilation vertex. Positive K mesons were identified by their decay (four events) and from bubble-density estimates; the K^- sample includes decays (three events), secondary interactions producing hyperons (five events), and those identified by bubble density of tracks.

With the numbers given in the seven event-type groups of Table II, it is in principle possible to determine both the detection efficiency for the K mesons,

TABLE II. Observed K-meson annihilation products.

	K^+	$K^+K_1^0$	K^+K^-	K^-	$K^-K_1^0$	K_1^0	$K_1^0K_1^0$
Neutron annihilation	6	2	3	4	4	9	0
Proton annihilation	10	1	3	13	7	11	3

and the branching ratios for the four reactions, i.e. those yielding $K^+\bar{K}^0$, K^-K^0, K^+K^-, and $K^0\bar{K}^0$. Such a procedure gave inconsistent results with the present data, presumably because of statistical fluctuations in this small sample. Instead, comparing the observed momentum distribution of charged K mesons with that for neutrals, we estimate the detection efficiency for K^+ and K^- to be $\epsilon_\pm = 0.5 \pm 0.2$. The stated error arises from the statistical uncertainty and a crude estimate of the effects of bias in identifying K mesons in the large "background" of pions and protons. For K^0 mesons we assume the detection efficiency to be simply the product of the probability of decay within the fiducial volume, $\epsilon_0 = 0.9 \pm 0.1$ and the branching ratio for $\pi^+\pi^-$ decay, 0.33. Thus we obtain the fractional rates for annihilations yielding K mesons,

$$R_k \text{ (deuterium)} = 0.059 \pm 0.011$$
$$R_k \text{ (protons)} = 0.064 \pm 0.014$$
$$R_k \text{ (neutrons)} = 0.051 \pm 0.013 \ .$$

These total branching ratios and the assumed detection efficiencies are consistent with branching ratios between 0.01 and 0.02 for each of the four modes above. Thus, the K-meson production rates, within the errors, are the same for proton and neutron annihilation.

Acknowledgments

We thank Professor Emilio Segré for continued support, much advice, and many illuminating discussions of the antiproton-annihilation process. Professor Kenneth M. Watson kindly provided us with the necessary formalism to make the final-state-interaction calculation. We are further indebted to Dr. Jonas Schultz for assistance in data analysis and for many helpful discussions. Our scanning and measuring crew, in particular Miss Gloria Tafralian and George Baker, performed with their usual industriousness and skill, for which we are grateful.

APPENDIX

Calculation of final-state interaction effects

We consider the annihilation reaction in deuterium yielding n pions and a proton. We assume that the proton is a spectator to the process of annihilation on the neutron in deuterium. The cross section for production of n pions with momenta in $d\underset{\sim}{q}_a$ and a proton with momentum in $d\underset{\sim}{Q}$ may be written, to within a normalization factor, as

$$d\sigma = \int \prod_{a=1}^{n} \frac{d\underset{\sim}{q}_a}{\omega_a} \frac{d\underset{\sim}{Q}}{E_Q} \delta\left(\sum_{a=1}^{n} \underset{\sim}{q}_a + \underset{\sim}{Q}\right) \delta\left(\sum_{a=1}^{n} \omega_a + E_Q - M_{\bar{p}} - M_d\right) |\mathcal{F}_{fi}|^2 ,$$

where ω_a, E_Q are the total energies of the ath pion and the proton, respectively, and $M_{\bar{p}}$, M_d are the antiproton and deuteron masses. The symbol $\mathcal{F}_{fi}$ represents the transition-matrix element between initial and final states. The momentum-space deuteron wavefunction may be factored from the matrix element --

$$|\mathcal{F}_{fi}|^2 = |\psi_d(Q)|^2 \, |F_{fi}|^2 .$$

The annihilation dynamics and the final-state-interaction effects are included now in the matrix element F_{fi}. Thus, the momentum distribution of the spectator proton that results is

$$P(Q) = |\psi_d(Q)|^2 \frac{Q^2}{E_Q} \int \prod_{a=1}^{n} \frac{d\underset{\sim}{q}_a}{\omega_a} \delta\left(\sum_{a=1}^{n} \underset{\sim}{q}_a + \underset{\sim}{Q}\right) \delta\left(\sum_{a=1}^{n} \omega_a + E_Q - M_{\bar{p}} - M_d\right) |F_{fi}|^2 .$$

Note first that with a statistical model—i. e. $|F_{fi}|^2$ is constant—the proton momentum distribution is not given by the deuteron momentum-space wavefunction, but is modified by the final-state phase-space factors. This is, of

course, a result of the requirement of overall energy-momentum conservation and is not a dynamical effect. Among the final-state interactions, only the π-p resonant interaction in the $T = 3/2$, $J = 3/2$ state is considered. Further, we neglect isotopic spin and construct the same enhancement factor for each pion, independent of the charge. We put then

$$|F_{fi}|^2 = \prod_{\beta=1}^{n} G(\omega_\beta),$$

where $G(\omega_\beta)$ is a weighting factor for the βth pion, due to the resonant final-state interaction. As given by GILLESPIE[12], these are

$$G(\omega_\beta) = \text{const} \times \exp\left\{\frac{2}{\pi}(\omega_\beta - \mu_\beta)\,\text{Princ}\int_{\mu_\beta}^{\infty} \frac{\delta(\omega')}{(\omega'-\mu_\beta)(\omega'-\omega_\beta)}\,d\omega'\right\},$$

where ω_β is the total energy, μ_β is the mass of the βth pion, and $\delta(\omega')$ is the phase shift for π-p scattering in the 3/2-3/2 state at pion energy ω'.

For present purposes a sufficient fit to the measured phase shifts is given by the function $\delta(\omega) = 2.31 \times 10^{-3}\,(\omega-\mu)^2$ for $\omega < 360$ MeV and $\delta(\omega) = 180\,[1-83.3/(\omega-\mu)]$ for higher energies. With these choices, the weight function $G(\omega)$ shown in Fig. 13 results. To calculate the proton-momentum distribution, we used a Monte Carlo technique for the particular state of five pions and recoil proton. Events were generated so that the momenta of all particles were distributed according to phase space only. Each event was then weighted by the value of the deuteron wavefunction squared for a proton of the given momentum, again with the deuteron wavefunction of ERIKSSON et al.[11]. The modified distribution so obtained was almost indistinguishable from the initial-state function $|\psi_d(Q)|^2 Q^2$ and so is not shown. To include the effect of final-state π-p interactions, as calculated above, we weighted each event by the

product of $|\psi_d(Q)|^2$ and the weights $\prod_{\beta=1}^{n} G(\omega_\beta)$ for the energies of the pions generated by the Monte Carlo technique. In Fig. 9 we show the histogram of events generated in this way, and for comparison the "Hulthén" distribution, together with the experimental results.

FOOTNOTES AND REFERENCES

*Work performed under the auspices of the U. S. Atomic Energy Commission.

†Now at Lawrence Radiation Laboratory, Livermore.

(1) Results on annihilation in nuclear emulsion are summarized in A. G. EKSPONG, Å. FRISK, S. NILSSON, and B. E. RONNE, Nucl. Phys. 22, 353 (1961).

(2) Annihilations in propane are discussed in LEWIS E. AGNEW, JR., TOM ELIOFF, WILLIAM B. FOWLER, RICHARD L. LANDER, WILSON M. POWELL, EMILIO SEGRÈ, HERBERT M. STEINER, HOWARD S. WHITE, CLYDE WIEGAND, and TOM YPSILANTIS, Phys. Rev. 118, 1371 (1960).

(3) NAHMIN HORWITZ, DONALD MILLER, JOSEPH MURRAY and ROBERT TRIPP, Phys. Rev. 115, 472 (1959).

(4) R. ARMENTEROS, L. MONTANET, D. R. O. MORRISON, S. N. NILSSON, A. SHAPIRO, J. VANDERMEULEN, CH. d'ANDLAU, A. ASTIER, J. BALLAM, C. GHESQUIERE, B. P. GREGORY, D. RAHM, P. RIVET, and F. SOLMITZ in Proceedings of the 1962 International Conference on High Energy Physics (CERN, 1962).

(5) Previous results, based on 34 events, are given in Ref. 3 above.

(6) P. BASTIEN, O. DAHL, and J. MURRAY, Proceedings of the International Conference on Instrumentation for High Energy Physics, Berkeley, 1960 (Interscience Publishers, N. Y., 1961).

(7) A. PAIS, Ann. Phys. 9, 548 (1960).

(8) J. SCHULTZ, Additional Conservation Laws in the Statistical Model for Meson Production (Ph. D. Thesis), Columbia University (1962) (unpublished). This paper includes references to other work on the statistical model.

(9) Y. YEIVIN and A. de SHALIT, Nuovo Cimento 1, 1146 (1955).

(10) G. B. CHADWICK, W. T. DAVIES, M. DERRICK, C. J. B. HAWKINS, J. H. MULVEY, D. RADOJIIČIĆ, and C. A. WILLIAMS, Phys. Rev. Letters, 10, 62 (1963).

(11) S. BERMAN and R. OAKES, Nuovo Cimento 29, 1329 (1963).

(12) B. ERIKSSON, L. HULTHÉN and N. JOHANSONS, Arkiv Fysik 25, 463 (1963).

(13) JOHN RAYMOND GILLESPIE, Final-State Interactions (Holden-Day, San Francisco, 1964); and The Effects of Final-State Interactions on Scattering Processes, (Ph. D. Thesis), Lawrence Radiation Laboratory Report UCRL-10762 (1963) (unpublished).

(14) T. A. GRIFFY and R. J. Oakes, Phys. Rev. 135, B1161 (1964). Other references are given here also.

FIGURE CAPTIONS

Fig. 1. Scatter plot of inverse of measured initial momentum versus observed length of each antiproton track which terminated in an annihilation event. The solid curve shows the expected behavior, deduced from the range-energy relation, for annihilations occurring at rest.

Fig. 2. Multiplicity distribution of the charged-pion prongs in 2071 antiproton-deuteron annihilations at rest. Events with identified K mesons are not included.

Fig. 3. Momentum distributions of (a) negative pions and (b) positive pions produced in antiproton-neutron annihilations yielding three charged pions. The smooth curves superimposed on the experimental histograms show the distribution given by Lorentz-invariant phase space.

Fig. 4. Momentum distributions of (a) negative pions and (b) positive pions produced in $\bar{p}$-n annihilations yielding five charged pions. The distributions given by Lorentz-invariant phase space are superimposed upon the experimental histograms.

Fig. 5. Effective mass of $\pi^+\pi^-$ pairs produced in $\bar{p}$-n annihilations yielding (a) three charged pions and (b) five charged pions. All possible $\pi^+\pi^-$ combinations were used for each event. The smooth curves show the distribution obtained from the statistical model.

Fig. 6. Distributions in χ^2 for (a) 39 events identified as annihilations yielding five charged pions and an unobserved missing π^0 and (b) 15 examples of five-charged-pion annihilations. The sample is restricted to events containing an observed proton spectator.

Fig. 7. Distribution of missing mass $\left(\sqrt{(\text{missing energy})^2-(\text{missing momentum})^2}\right)$ in 67 examples of $\bar{p}$-d annihilations yielding five charged pions and a proton spectator. Identification of the number of missing π^0's is shown by the appropriate shading in the histogram.

Fig. 8. Momentum distribution of observed, identified proton-spectator tracks resulting from $\bar{p}$-d annihilations into three and five charged pions. The smooth curve is the nucleon internal-momentum distribution obtained from a "Hulthén" deuteron wavefunction.

Fig. 9. Observed momentum spectrum of proton spectators in $\bar{p}$-d annihilations into three and five charged pions compared with a calculated distribution in which the resonant pion-proton interaction in the final state of five pions and a proton was taken into account. The latter is shown in the dotted histogram, a result of a Monte Carlo calculation. For comparison, the "Hulthén" spectrum is shown also

Fig. 10. Calculated momentum spectrum of protons resulting from decay of $N^*(1238)$ produced in the annihilation reaction $\bar{p}$-d $\rightarrow N^* + 4\pi$ proceeding according to the statistical model. The N^* decay is assumed isotropic in the N^* rest system.

Fig. 11. Effective mass of (a) $p\,\pi^-$ and (b) $p\,\pi^+$ pairs of particles produced in the antiproton annihilations on deuterium yielding three and five charged pions in the final state with an identified proton-spectator track.

Fig. 12. Phase-space distribution of momentum of protons produced in the assumed annihilation reaction $\bar{p} + d \rightarrow 5\pi + p$.

Fig. 13. Weighting factor enhancing the yield of pions, in $\bar{p}$ d annihilations, at momenta near that of the final-state π-p resonant interaction.

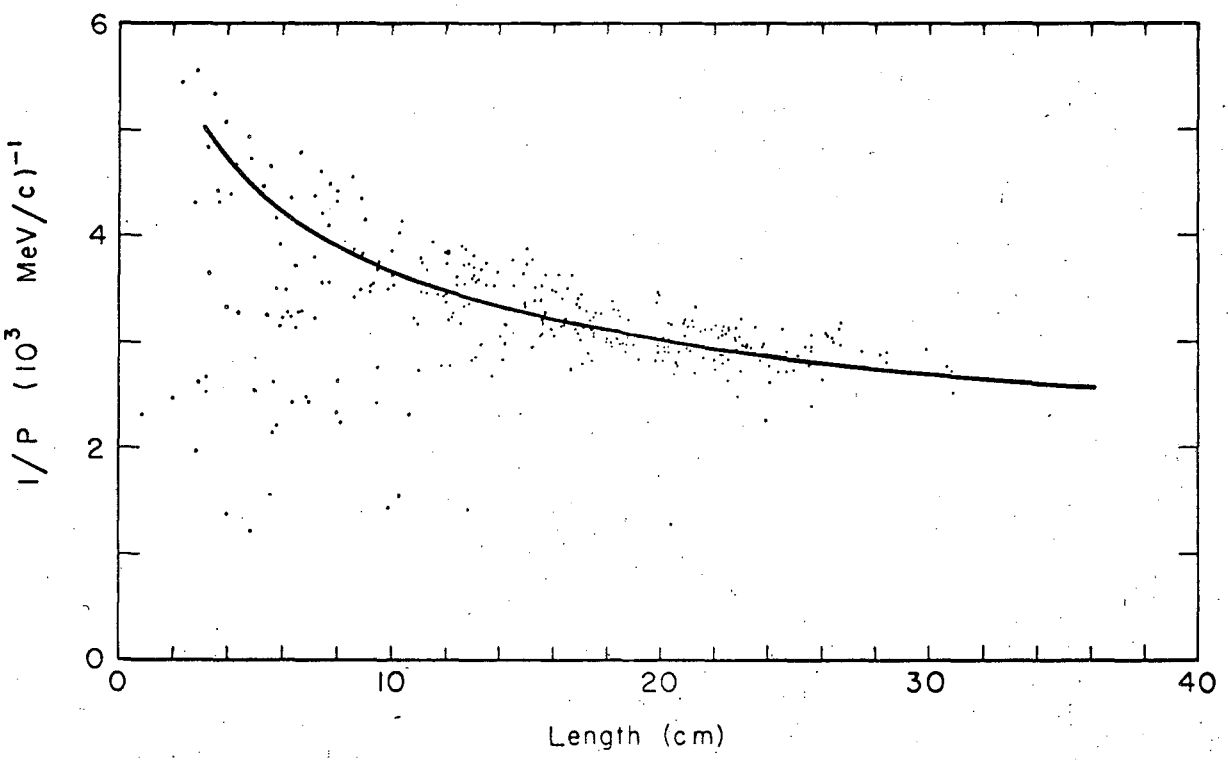

Fig. 1

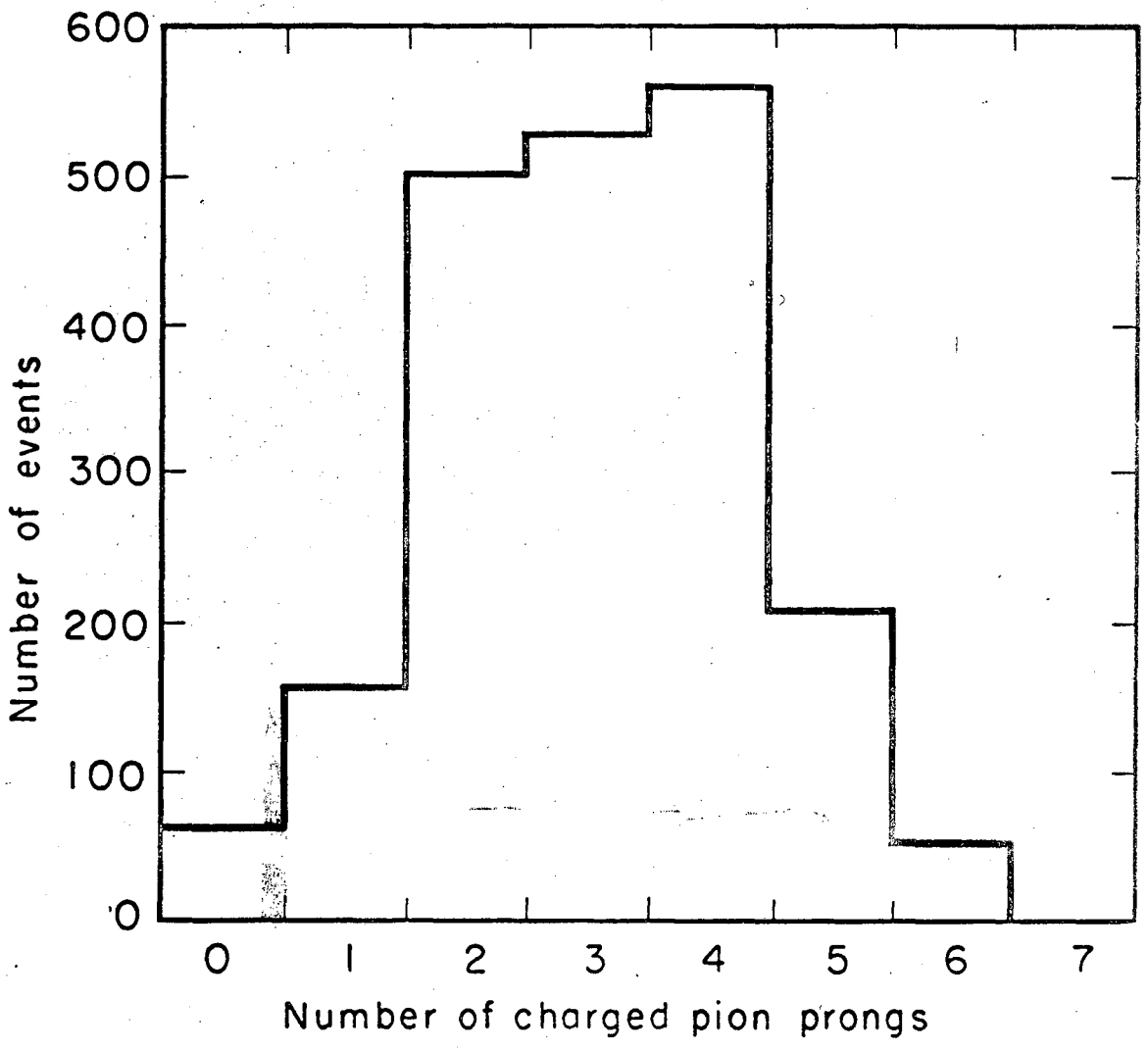

MUB-7714

Fig. 2

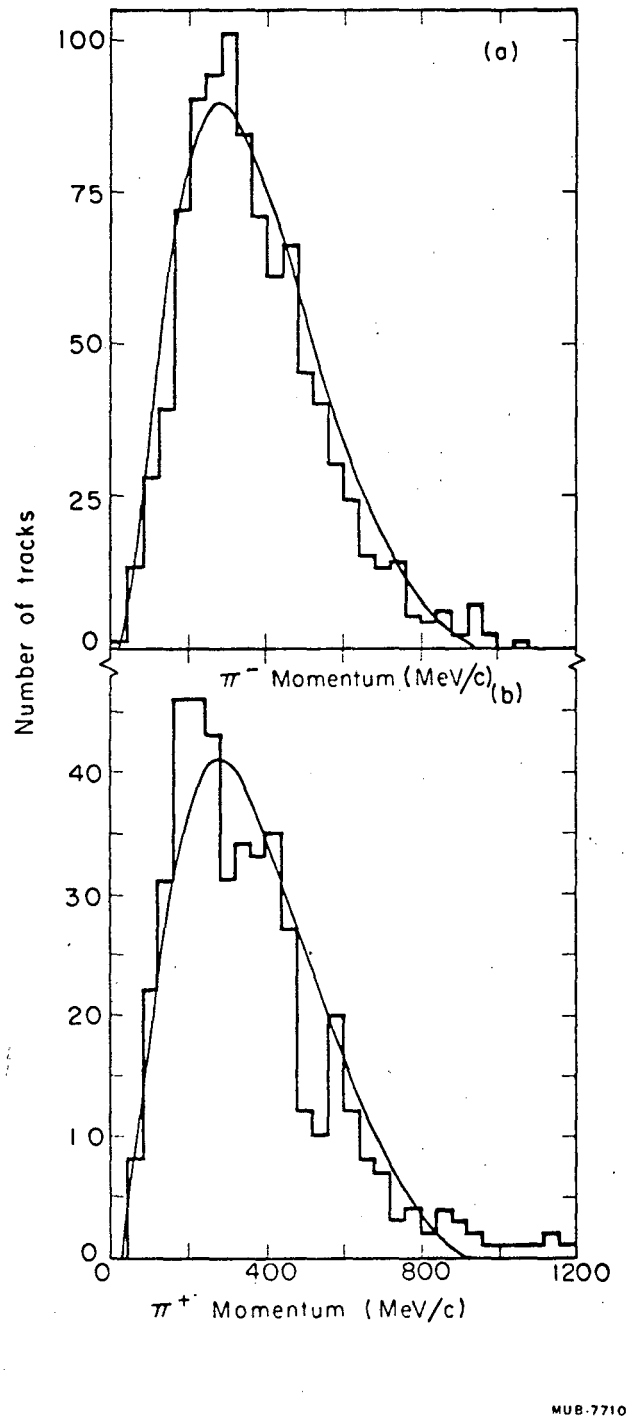
100
75
50
25
0
(a)
Number of tracks
π^- Momentum (MeV/c)
(b)
40
30
20
10
0
0
400
800
1200
π^+ Momentum (MeV/c)
MUB-7710

Fig. 3

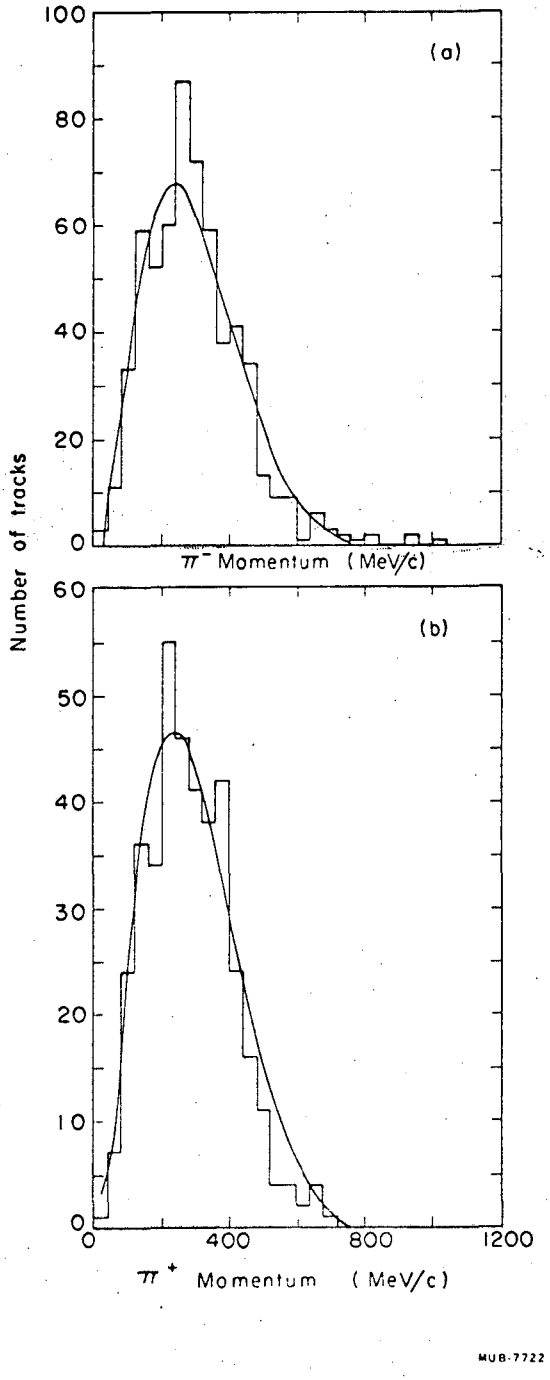
(a)
(b)
Number of tracks
π^- Momentum (MeV/c)
π^+ Momentum (MeV/c)
0
20
40
60
80
100
10
30
50
400
800
1200
MUB-7722

Fig. 4

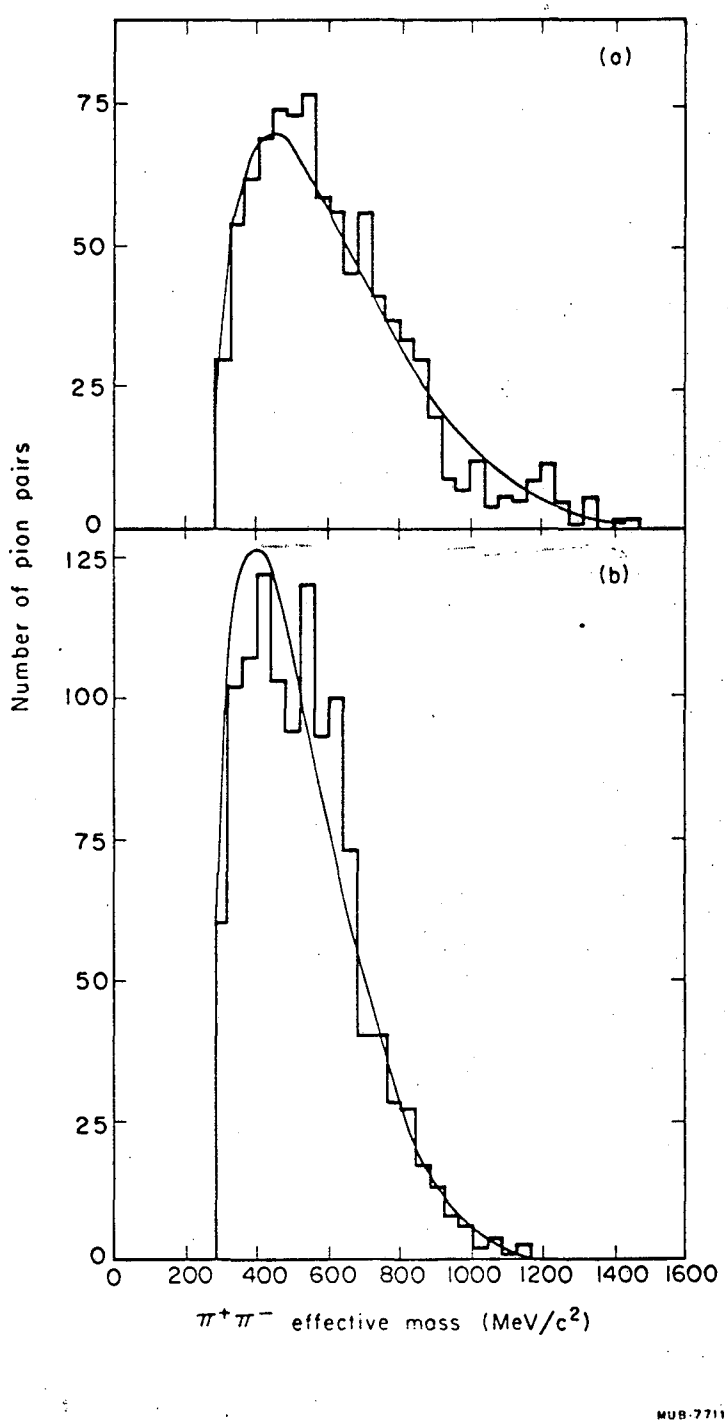
(a)
(b)
75
50
25
0
125
100
75
50
25
0
Number of pion pairs
0
200
400
600
800
1000
1200
1400
1600
$\pi^+\pi^-$ effective mass (MeV/c^2)
MUB-7711

Fig. 5

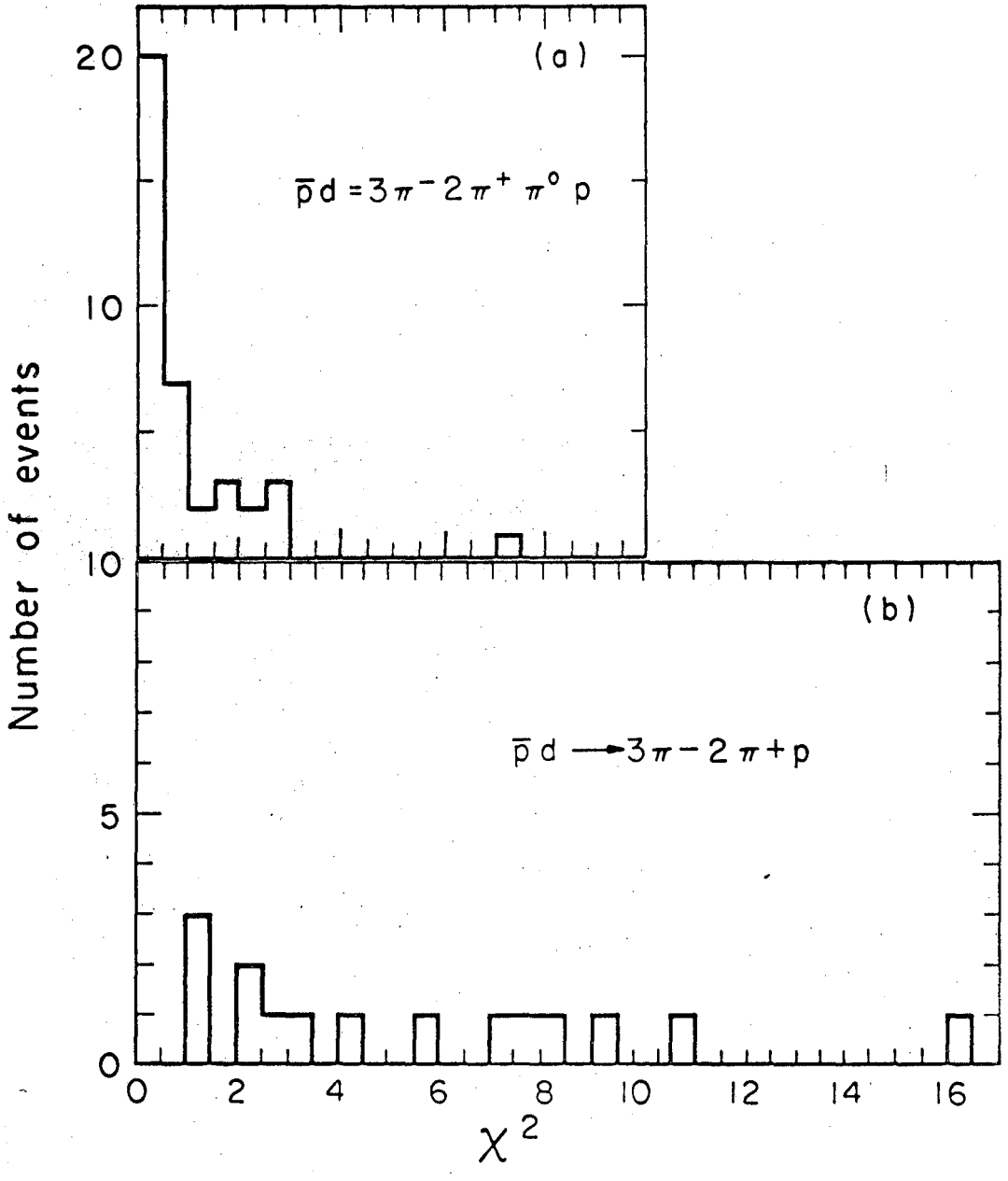

MUB-7720

Fig. 6

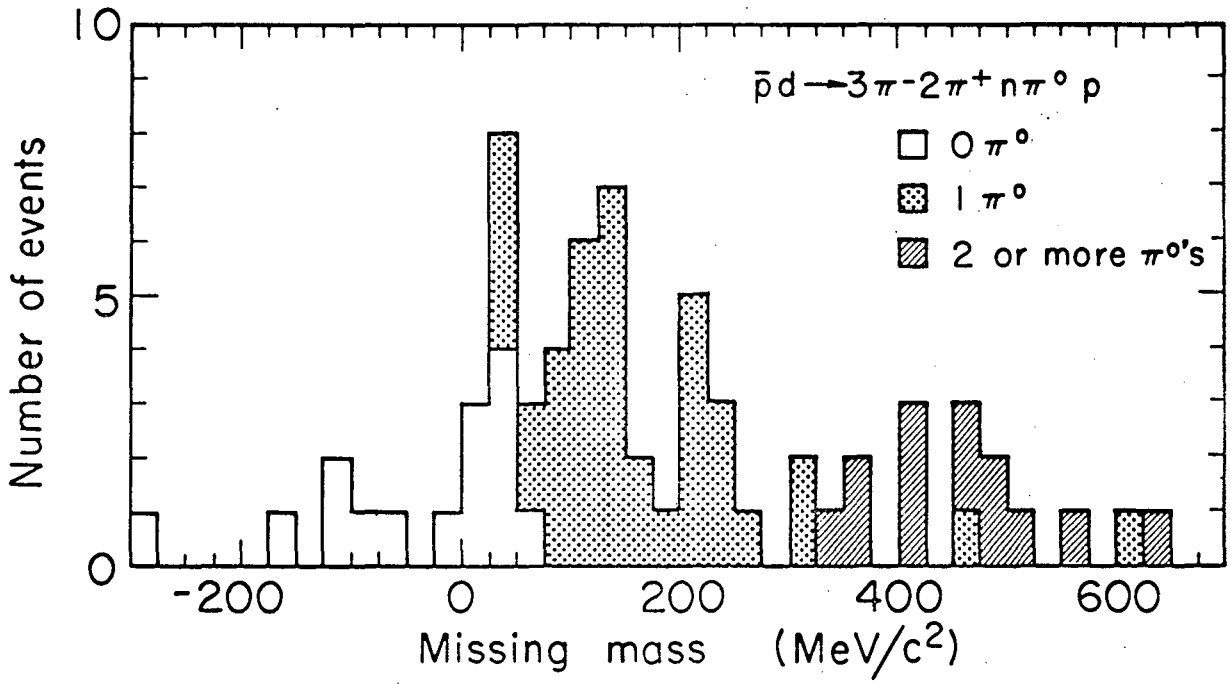

MUB-7719

Fig. 7

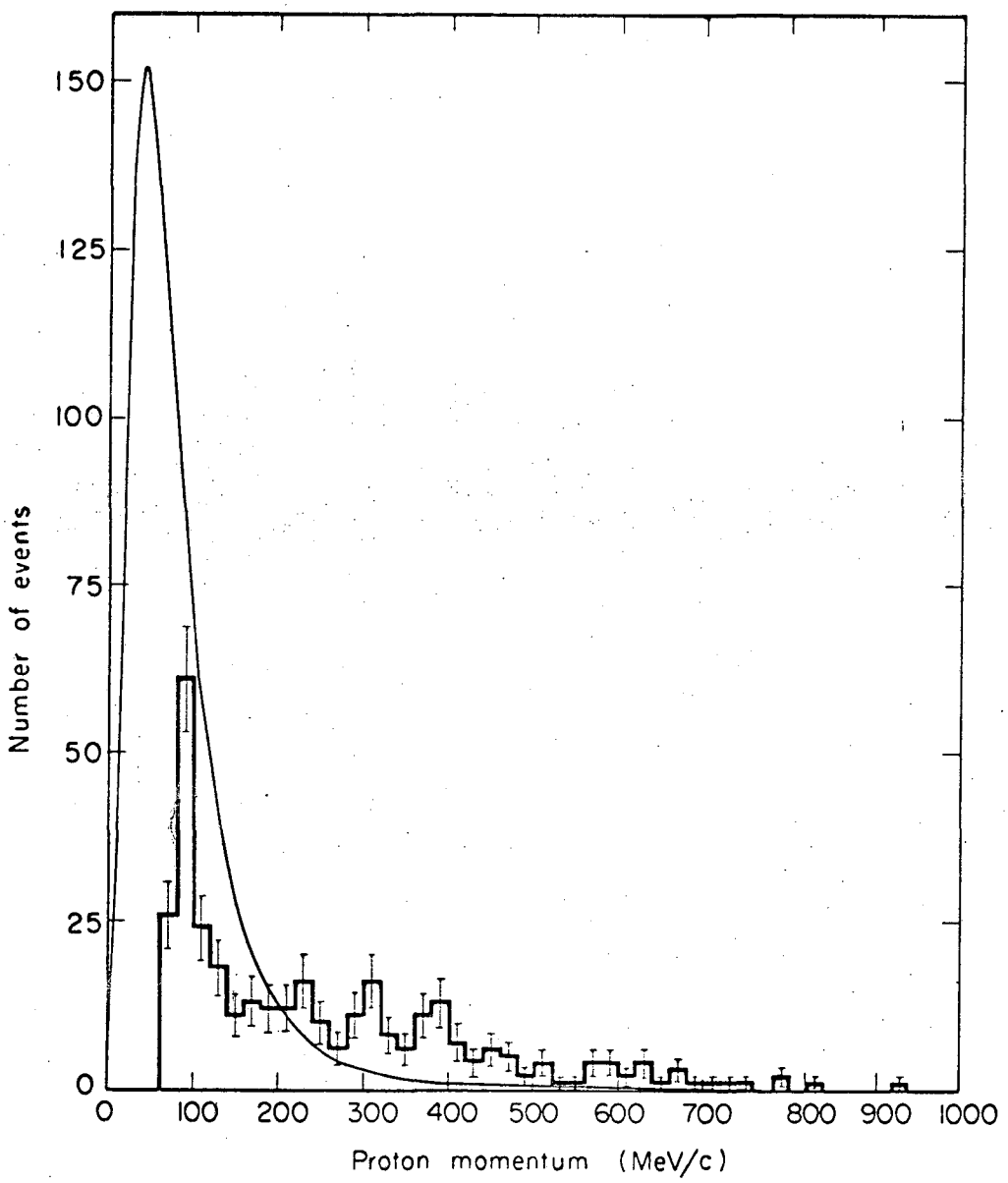
150
125
100
75
50
25
0
Number of events
0
100
200
300
400
500
600
700
800
900
1000
Proton momentum (MeV/c)
MUB-7718

Fig. 8

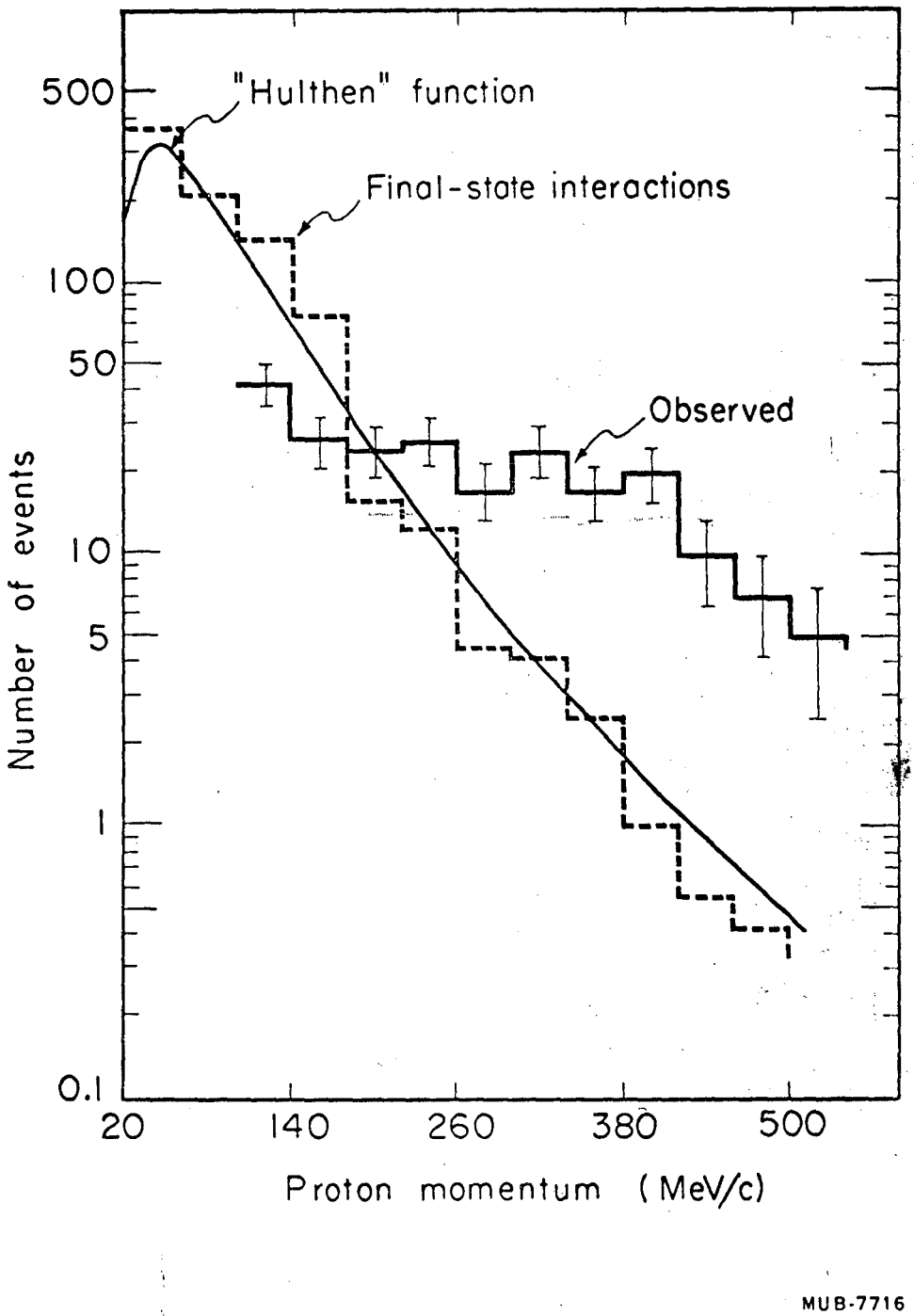
"Hulthen" function
Final-state interactions
Observed
Number of events
500
100
50
10
5
1
0.1
20
140
260
380
500
Proton momentum (MeV/c)
MUB-7716

Fig. 9

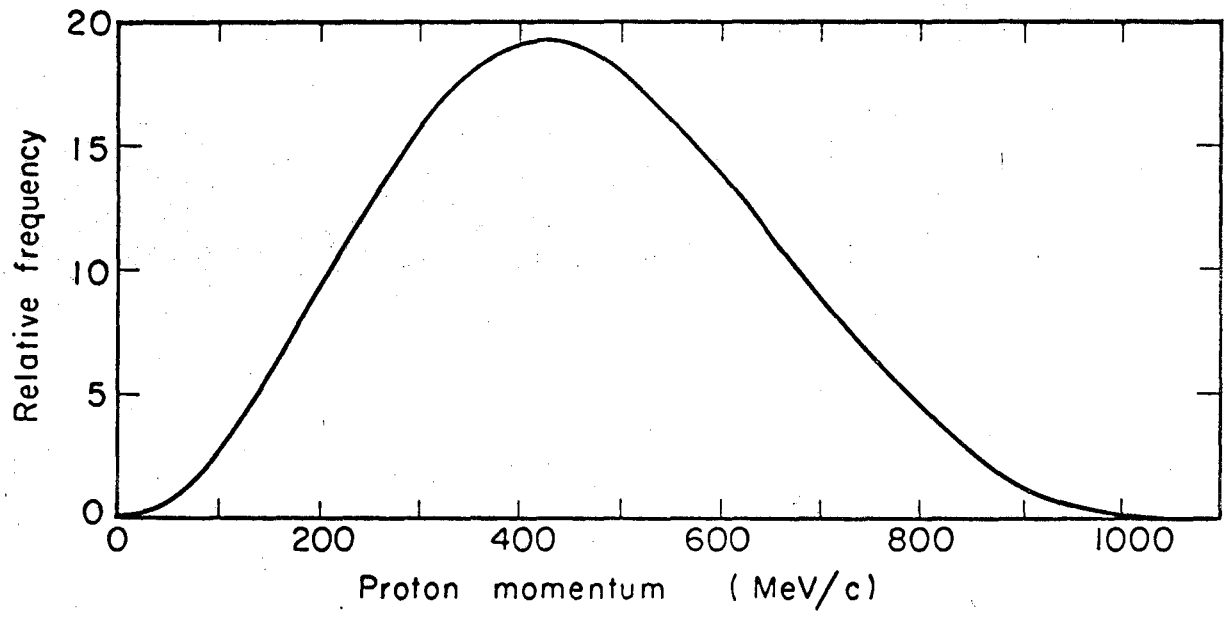

MUB-7713

Fig. 10

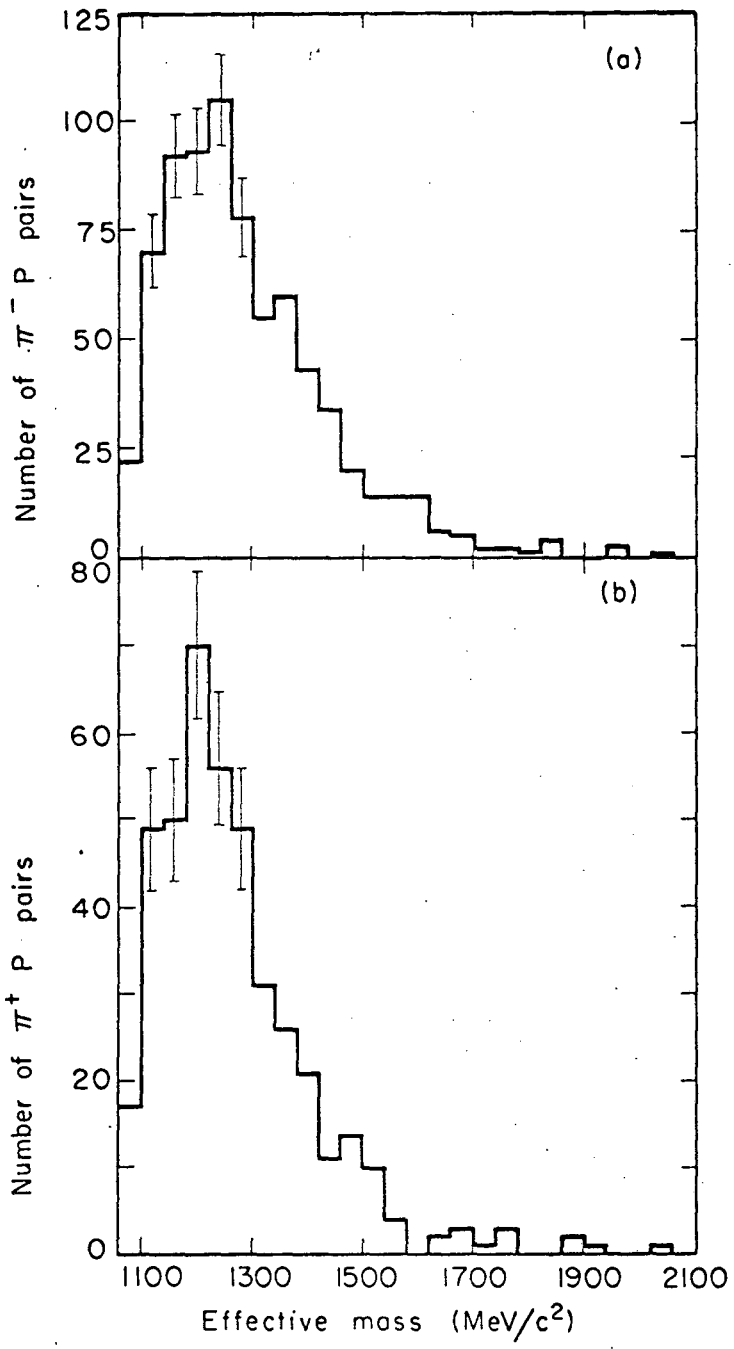
125
100
75
50
25
0
(a)
Number of π^- P pairs
80
60
40
20
0
(b)
Number of π^+ P pairs
1100
1300
1500
1700
1900
2100
Effective mass (MeV/c^2)
MU8-7712

Fig. 11

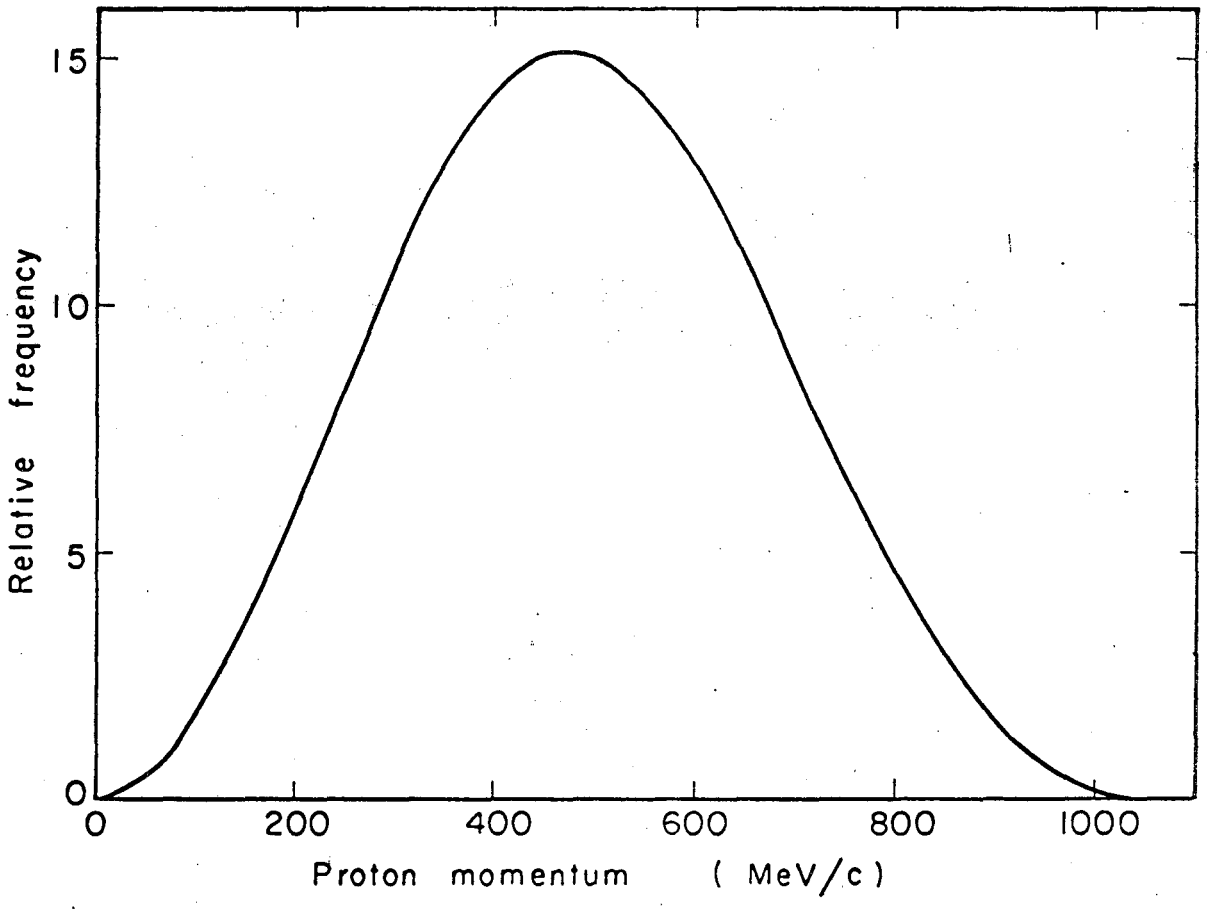

MUB-7715

Fig. 12

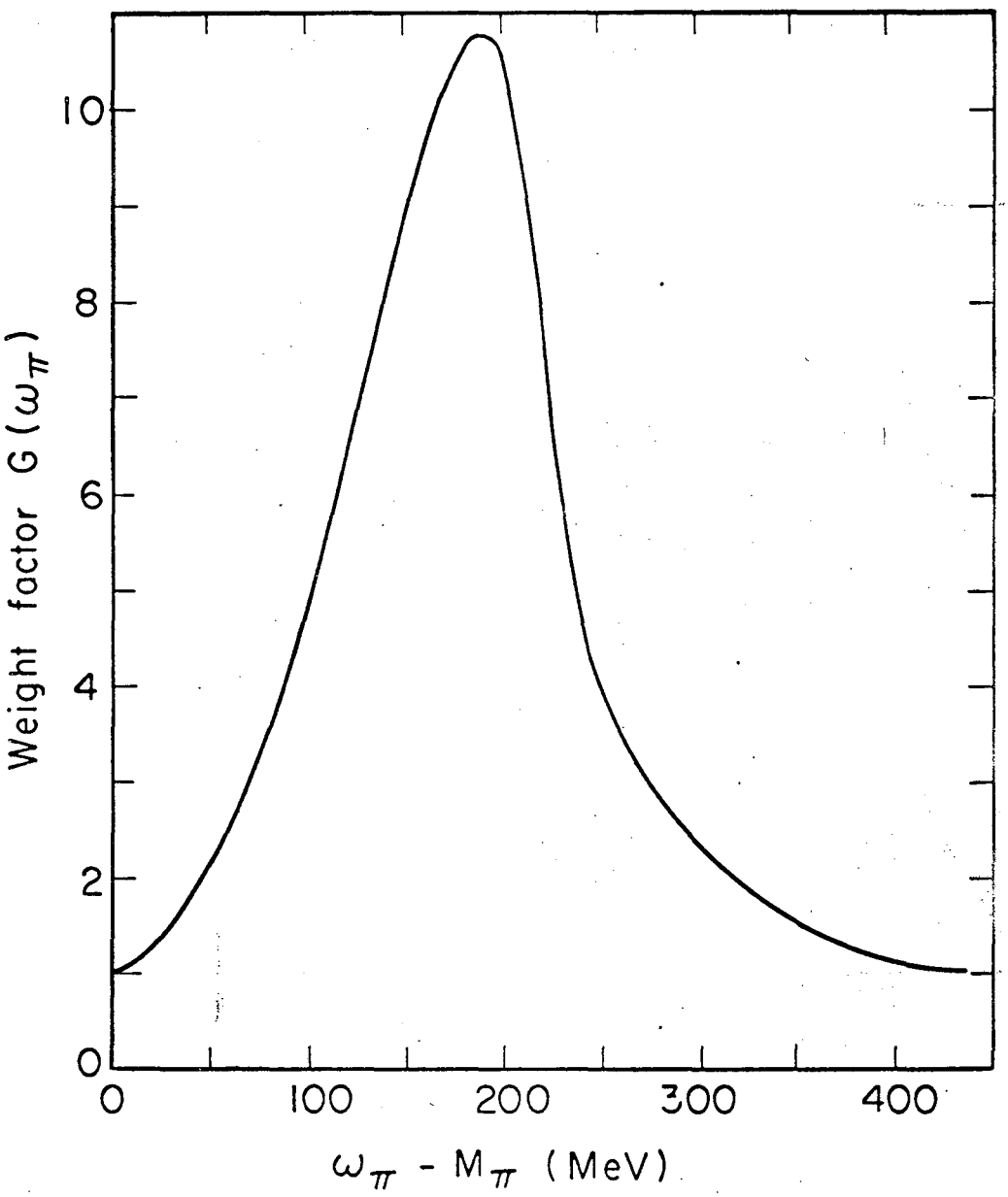
Weight factor $G(\omega_\pi)$
0
2
4
6
8
10
0
100
200
300
400
$\omega_\pi - M_\pi$ (MeV)
MUB-7717

Fig. 13